

## NUMERICAL STUDY OF CAROTID BIFURCATION ANGLE EFFECT ON BLOOD FLOW DISORDERS

N. Lewandowska\*, M. Micker<sup>†</sup>, M. Ciałkowski\*, M. Warot<sup>†</sup>, A. Fraćkowiak\*, P. Chęciński<sup>†</sup>

\*Poznan University of Technology  
Faculty of Machines and Transport  
Chair of Thermal Engineering  
Piotrowo 3, 60-695 Poznan, Poland  
natalia.lewandowska.pp@gmail.com

<sup>†</sup> Poznan University of Medical Sciences (PUMS),  
Department of General and Vascular Surgery and Angiology  
34 Dojazd St, 60-631 Poznan, Poland  
maciej.micker@wp.pl

**Keywords:** Biomechanics, Biomedical Engineering, Computational Fluid Mechanics, carotid artery, bifurcation angle, internal carotid artery, external carotid artery, non-Newtonian fluid, atherosclerosis, numerical modeling, CFD

**Abstract:** *The paper presents study results of the impact of the common carotid artery bifurcation angle on the flow disorders. The studies were carried out using numerical methods. Based on actual images, geometry was made of the diffuser channel with bifurcation and predetermined angle. The flow simulation results showed that for bifurcation angles exceeding 60° the whirlpools near the bulb start to occur – at that time almost a double increase of the parameter values takes place, related to flow disorders. The whirlpools become increasingly larger and grow proportionally to the value of the bifurcation angle. Thanks to the studies carried out, three areas have been shown, in which plaques may deposit, due to disadvantageous geometry. Based on the simulation results, arteries have been divided into three groups of risk. It has been proven that bifurcations exceeding 50 degrees significantly disturb the flow and the points of whirlpool occurrence represent frequent points of plaque depositions.*

## 1 INTRODUCTION

This paper presents the study results aimed at the determination of anatomy of carotid arteries with geometry enhancing plaque deposition. The application of numerical methods in medicine becomes increasingly popular. There are vascular surgery issues that, in addition to biological (physiological), have a mechanical (haemodynamic) cause. Thanks to the combination of the two fields of science, the phenomena occurring in the artery can be explained more completely. Through analysis of the flow field in the common carotid artery bulb, the phenomenon of boundary layer separation and formation of whirlpools can be detected. If the whirlpool occurring in the flow is sufficiently large and strong, it causes a 'suction' of solids present in the blood such as components of atherosclerotic plaque. As a result, the said particles deposit on the arterial walls. They will cause a progressive stenosis, which enhances the process of further formation of vortices (Fig. 1). This is one of the theories of atherosclerotic plaque formation in the point or arterial bifurcation.

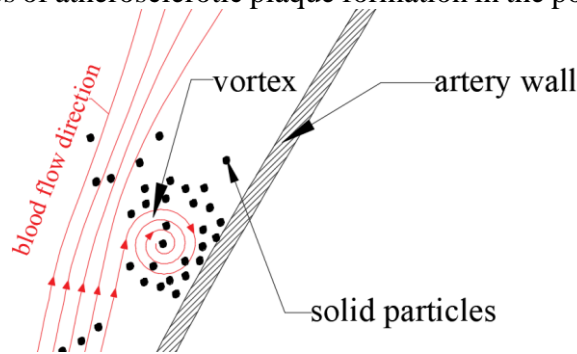


Figure 1: Deposition of solid particles following the vortex formation.

The literature [1-6] concerning numerical studies of carotid arteries presents studies mainly focused on carotid artery thicknesses and diameters of the cross-section of its branches. The analysis was mainly carried out through presentation of the shearing stress field and the velocity values in the canal. It was shown that arterial narrowing leads to increased blood flow velocity and, as a consequence, growth of the shearing stresses, which enhances flow turbulization and affects formation of deposits. In addition, weakening of the arterial walls caused by lesions in the patient causes reduced flexibility of the wall and local expansion of internal carotid artery, which also causes deposition of atherosclerotic plaques and may also cause their formation. The deposits most often occur on the side of the internal carotid artery, which is particularly dangerous, because this artery transports blood to the brain and its closing very often causes irreversible damage to the cerebral tissue or even death.

The formation of deposits on the side of the internal carotid artery is, most of all, enhanced by its geometry – the increasing cross-section of the flow causes a reduction of the blood flow and, as a consequence, its increased viscosity, which has been explained in detail further in the paper. High viscosity enhances the formation of deposits, because separation of the boundary layer occurs near the walls and vortices occur more easily. Except the aspects directly concerning the geometry of the specific arteries, the parameters correlating the external and internal carotid artery are also significant.

Bulb is the key region, in which the blood flow is most exposed to disorders – this is the area where the artery expands and is bifurcated into two smaller arteries (Fig. 2).

In contrast to the previous analyses in this field, the authors decided to focus on one though very important parameter, differentiating the carotid arteries. This is the bifurcation angle of the common carotid artery. This paper will include studies on the impact of the change of the said angle on the blood flow parameters. It is rarely considered in blood flow analyses, though it expressly enables the determination of some groups of carotid arteries with geometry enhancing the formation of deposits. From the flow point of view, the area distinctly changes such parameters as flow velocity, pressure and, most importantly, stability. The purpose of the studies was to check, with the use of numerical methods, whether vortexes would occur with correspondingly large bifurcation angles, which, as a consequence might lead to the formation of deposits. The purpose of the study was to determine geometrically correct arteries. The practical result of the studies is the possibility to apply proactive measures aimed at the delay or reduction of the risk of deposits formation in patients with arteries classified within the risk group.

## 2 METHODS

The studies were carried out using the ANSYS software, through numerical modeling of the flow. The CFD (*Computational Fluid Dynamics*) tools enable a very good reproduction of the flow, if appropriate number of parameters is included in the model. Fig. 2 presents a general outline of geometry made in AutoCAD. The CCA (*Common Carotid Artery*) was treated as a non-symmetric diffuser canal. Based on the analysis of real images of arteries and papers treating on carotid artery studies [1-6], it was observed that the bifurcation of the ICA (*Internal Carotid Artery*) is by ca.  $5^\circ - 10^\circ$  larger than the bifurcation of the ECA (*External Carotid Artery*). The ICA and ECA were also approximated as straight-line canals. The main area of study – the bulb, was distinguished in Fig. 2c. The increased length of the canals results from the fact that laminar stabilized inlet and outlet flows were targeted during the simulation.

The most important aim of the studies was the watch of the boundary layer separation and the formation of the vortex. The accuracy of detection of the said phenomena is determined by the turbulence models. For each case, depending on the flow conditions and parameter values, an individual model should be selected. After a detailed analysis, the  $k-\omega$  SST model was selected, which perfectly reproduces the points of the boundary layer separation [8,9].

The boundary conditions define the velocity or the pressure values in the artery flow inlets and outlets. The velocity value was selected based on actual values occurring in the common carotid arteries [8,9] equaling to 1 m/s. At the arterial flow outlets, the zero-pressure boundary condition was applied to settle the zero overpressure value at the outlets. The condition is particularly often applied in the cases where the most important study parameter is the nature of the flow [4,6].

In reality, the arterial blood flow is of a pulsating nature. In the studies, a stationary flow with constant velocity profile at the inlet (constant in time) was applied. The simplification is reasonable, because the authors' main focus was the impact of the geometry on the nature of the flow.

The blood flowing through the carotid arteries is an untypical fluid, referred to as the non-Newtonian fluid. It differs from Newtonian fluids by the fact that its viscosity is not a constant value. Viscosity is a physical value included in the description of a relation between the shearing stresses occurring in fluid  $\tau$  and the fluid velocity gradient  $u$  along normal direction to the surface of occurrence of the shearing stresses  $x_i$  (referred to as the non-dilatational strain velocity) [12]. High viscosity fluids are characterized with the fact that with low velocities even the boundary layer might be separated and strong flow disorders might occur. Blood is a

pseudo-plastic fluid and its viscosity reaches high values at low velocity, however, the faster it flows in the artery the lower the viscosity. The Carreau model [4,6,10,11] was used to create the blood model (equation (1)). In contrast to other, less complex models, it implements the value referred to as the fluid relaxation time, which causes a delay of viscosity drop as a result of the strain velocity growth and is milder, which reflects the nature of the pseudo-plastic fluid and the viscosity value in the area of low shearing velocities. It leads to a higher effectiveness of detection of the boundary layer separations.

The values of the coefficients in relation [1] were selected based on the paper, in which they were determined following a series of experiments [6].

$$\mu_{\text{eff}}(\dot{\gamma}) = \mu_{\infty} + (\mu_0 - \mu_{\infty}) \left(1 + (\lambda \dot{\gamma})^2\right)^{\frac{n-1}{2}} \quad (1)$$

of which:

$$\dot{\gamma} = \frac{\partial u_i}{\partial x_i} \left[ \frac{1}{s} \right] - \text{strain velocity}$$

$\lambda = 3.13 \text{ s}$  – fluid relaxation time

$n = 0.3568$  – exponent

$\mu_{\infty} = 0.00345 \text{ kg/m}\cdot\text{s}$  – viscosity value at infinitely high shearing velocity (in the flow core),

$\mu_0 = 0.056 \text{ kg/m}\cdot\text{s}$  – viscosity value at zero shearing velocity (near the walls).

Upon the analysis of the actual images of the arteries, the range of angles between the external and internal carotid arteries occurring in reality was determined. The value of the smallest bifurcation angle is  $15^\circ$ , while the largest bifurcation detected was  $90^\circ$ . To analyze the flow at various angles, 9 models of the following angle values have been made:  $15^\circ$ ,  $30^\circ$ ,  $40^\circ$ ,  $45^\circ$ ,  $50^\circ$ ,  $55^\circ$ ,  $60^\circ$ ,  $75^\circ$  and  $90^\circ$ . It was observed that from  $40^\circ$  to  $60^\circ$  the angle was changed every  $5^\circ$ , because in this area, the first larger separations were expected. To assess the flow nature, the authors considered the following factors while developing the results:

- a) the boundary layer thickness in the diffuser part and at the outlets  $\delta$  [mm]: the value was assessed by determining the areas, in which the fluid velocity was lower than in the flow core. In Fig. 3, a concept of measurement was presented based on the example of one of the outlets. According to the common assumption, the boundary layer occurs until the flow velocity reaches 99% of the core flow value [12];

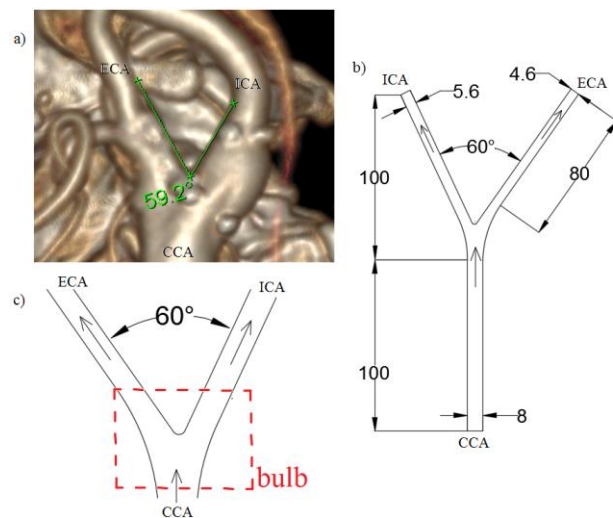


Figure 2: Carotid artery: a) real b) geometric model c) bulb.

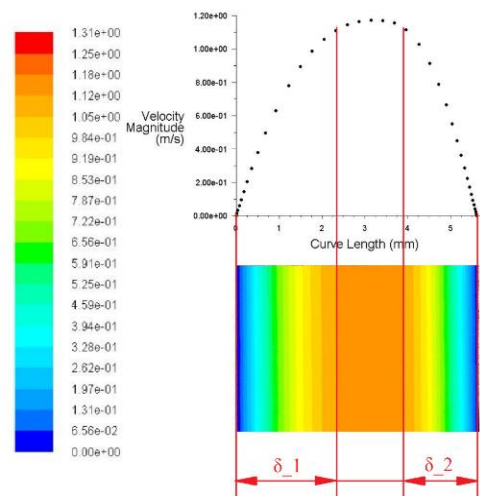


Figure 3: Measurement of the thickness of the boundary layer

b) turbulent Reynolds number  $Re_{turb}$  [-], which defines the turbulent viscosity (defined by Boussinesq function) to laminar viscosity ratio [7]. The probability of occurrence of vortices and separations grows along with the value of the turbulent Reynolds number in a specific area.

c) kinetic energy of turbulence  $k$  [J/kg] – average kinetic energy referred to mass unit and related to the vortices in the turbulent flow. When the flow becomes turbulent, the share of diffusion in the transport grows. It was assumed that the turbulent flow structure contains areas of highly non-stationary nature, referred to as vortices. The intensification of vortices increases the transportation of volumes by diffusion – they can be small or large. The kinetic energy of turbulence is the energy of vortices in a turbulent flow – the larger they are the more their kinetic energy grows. It is ‘supplied’ from the kinetic energy of flow to larger vortices, from larger to smaller to dissipate in the end – until the vortices are so small that the viscosity forces overcome the inertia forces (correlated with kinetic energy). When assessing the field of the kinetic energy of turbulence, one can locate the area of the vortex occurrence and referring the value of the said energy to the kinetic energy of fluid, one can estimate what part of the kinetic energy related to laminar flow is transformed into turbulence energy.

### 3 RESULTS

Three possible areas occur in the artery, in which, due to the reduction of velocity (i.e. also increase of viscosity) deposits in the form of atherosclerotic plaques may occur. Fig. 4b shows the field of turbulent Reynolds number  $Re_{turb}$ , which defines the ratio of turbulent viscosity (defined by Boussinesq function) to laminar viscosity [7]. The probability of vortices and separations grows along with the turbulent Reynolds number in a specific area. The graphical presentation precisely shows that the areas of high  $Re_{turb}$  correspond to the locations of deposits [11].

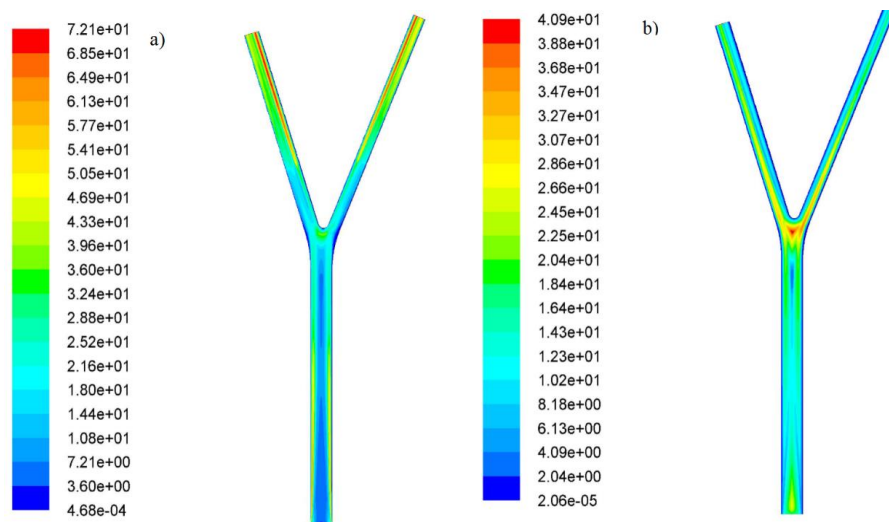


Figure 4: Distribution: a) Reynolds number b) turbulent Reynolds number (case: 40 °)

Allowing for the kinetic energy of turbulence  $k$  in the cases presented in the analysis, the areas of the highest value of this energy occur in the bulb, in the vicinity of the walls (Fig. 5). For the smallest angle, the energy is  $0,0086 \frac{J}{kg}$ , while for the angle of  $90^\circ$  it is  $0,0192 \frac{J}{kg}$ , i.e. a more than double growth of kinetic energy of turbulence is detected. In the case of wider angles, a strong growth around the external artery wall takes place, because the vortex is formed at this point.

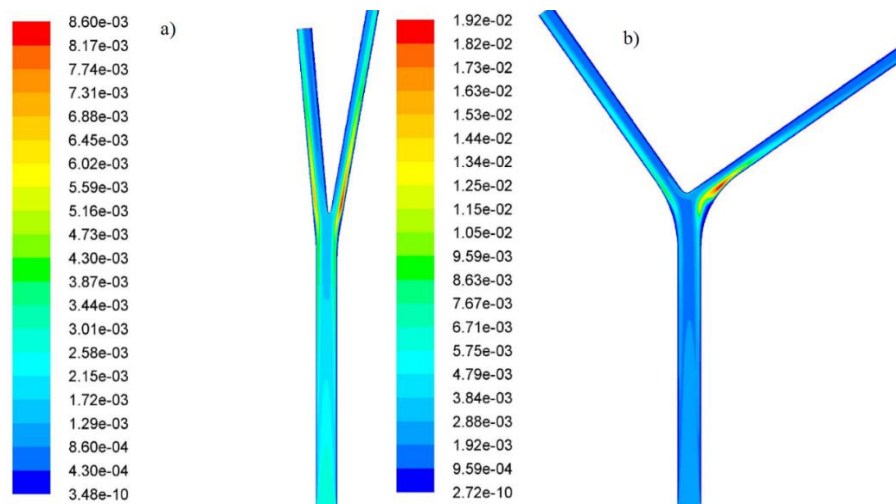


Figure 5: Turbulence kinetic energy distribution  $k$  [J / kg] a) angle of  $15^\circ$  b) angle of  $90^\circ$

The greatest thickness of the boundary layer occurs in the area, in which the straight-line canal starts to diverge. The increase of the cross-section, which the fluid flows through causes a drop of pressure, which enhances the separation of the boundary layer. Along with the angle growth, the thickness of the boundary wall grows. Fig. 6 presents the field of velocity for the bifurcation angle of  $15^\circ$ ,  $50^\circ$  and  $90^\circ$ . It was observed that the angle growth causes the growth of the separation area, which is the place of the deposit formation, especially on the side of the internal artery [12].

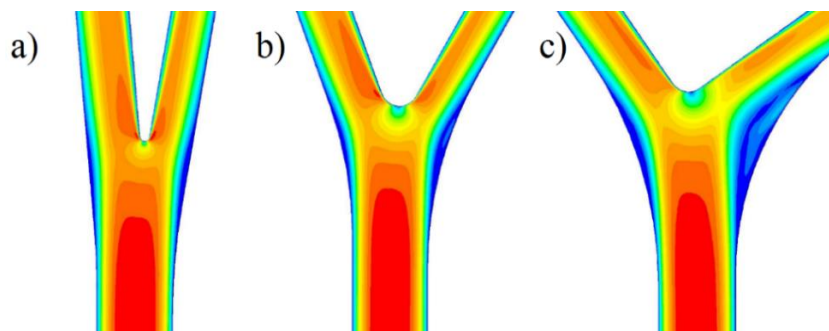


Figure 6: Velocity field for the angles of: a)  $15^\circ$  b)  $50^\circ$  c)  $90^\circ$

From the angle of  $60^\circ$  in the area of the increase of the cross-section, low velocity vortices appear, which is shown by the curve of current line (Fig. 7a). It was observed that the vortices did not occur at the angle of  $55^\circ$  and, upon changing of the bifurcation angle by  $10^\circ$ , a rapid growth of the kinetic energy of turbulence (from 0.0105 to 0.016 J/kg), turbulent Reynolds number (from 43.3 to 71.6) and the boundary layer thickness (from 2.5 mm do 3.7 mm) were observed. Such flow retreat, even in the low velocity area, is very dangerous, because it enhances the deposition of atherosclerotic plaques and other solid particles near the walls. The larger the angle, the larger the area of the formed vortex. (Fig. 7b), and, as a consequence, the flow structure becomes increasingly distorted. In addition, with reduced velocity, the viscosity of blood as a fluid thinned with shearing is very high, which impedes the laminar flow through the arteries. These two factors – the boundary layer and the increased viscosity have the greatest impact on the nature of the flow.

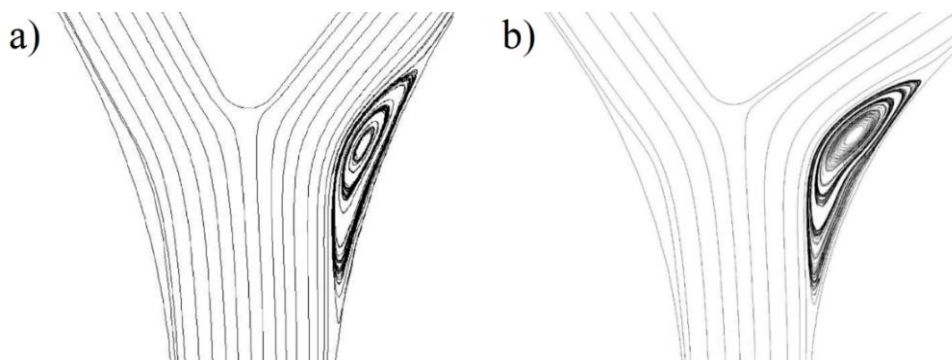


Figure 7: Pathlines of flow for angle of: a) 60° b) 90°

Fig. 8 presents the velocity profiles at the outlet from the canals and the profile of velocity distribution in the ICA with the angles of 15° and 90°. The non-symmetrical nature right at the outlet from the bulb results from the earlier flow deceleration at the stagnation point. At the angle of 90°, a separation of the boundary wall occurs along with a clear impact of the stagnation point on the maximum value of velocity in the diffuser part of the canal.

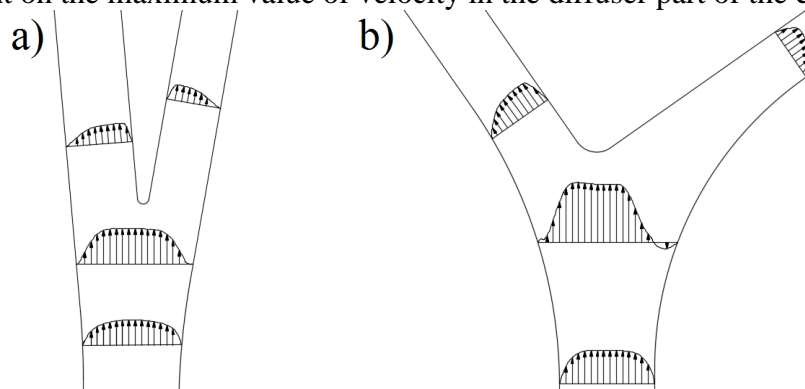


Figure 8: Velocity profiles a) angle of 15° b) angle of 90°

## 5 CONCLUSIONS

The angle between the external carotid artery and the internal artery has the greatest impact on the following factors and phenomena: thickness of the boundary layer, place of inflows of the concentration point and formation of vortices (separation and flow retreat). The larger the areas of plaque deposition, the wider the angle between the arteries. The following phenomena occur in the said zones:

- the velocity (kinetic energy) decreases;
- the turbulent Reynolds number and the kinetic energy of turbulence reach the maximum (at the cost of the decrease of the kinetic energy related to laminar flow);
- separation of the laminar layer and flow whirlpool occur – for angles wider than 60°;
- the viscosity grows (caused by decreased velocity);
- the impact of the concentration point on the velocity profiles at the outlets (thicknesses of the boundary layers) grows, because it causes acceleration of the fluid in the areas behind the stagnation point. This area is additionally beneficial in terms of plaque deposition.

Based on the above prerequisites, the simulation results were divided into three principal

groups. Figures 9-11 present a series of diagrams reflecting the following relations: boundary layer thicknesses, kinetic energy of turbulence and turbulent Reynolds number, depending on the carotid artery bifurcation angle. A fast growing trend of the above parameters for angles above 50° is particularly distinct.

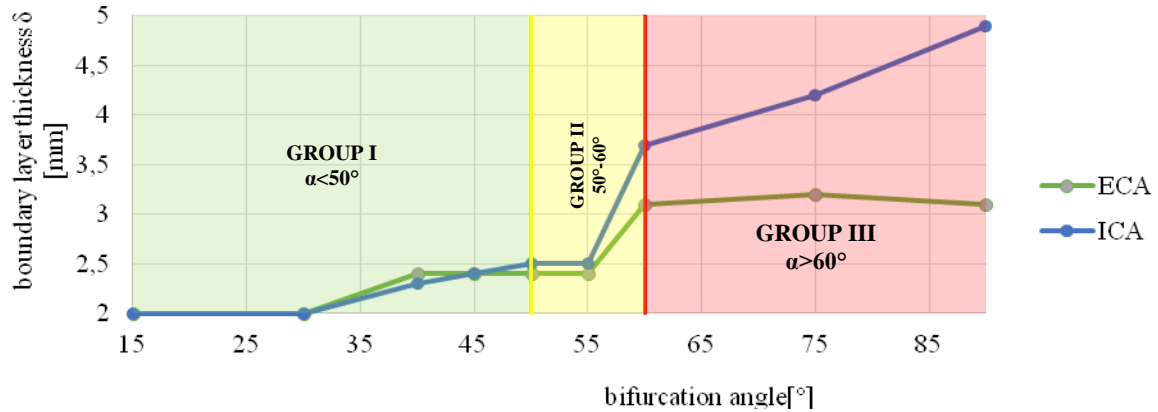


Figure 9: Thickness of the boundary layer as a function of the bifurcation angle

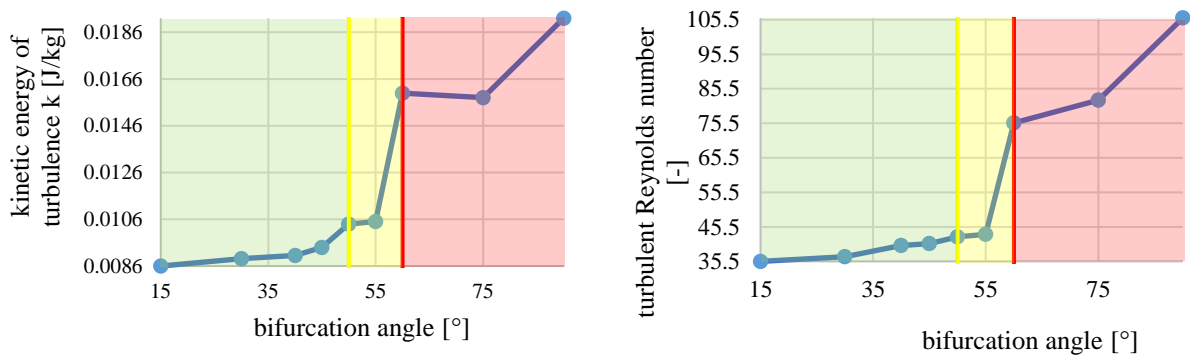


Figure 10: Kinetic energy of turbulence as a function of the bifurcation angle

Figure 11: Turbulent Reynolds number as a function of the bifurcation angle

**GROUP I: angles below 50°** → carotid arteries of geometries that cause no flow disorders, the change of value in the angle function is relatively constant.

**GROUP II: angles in the range 50°-60°** → carotid arteries, in which the parameters related to the flow turbulence grow, but no vortex flows appear.

**GROUP III: angles above 60°** → carotid arteries of geometries enhancing the deposition of plaques with a tendency to separation and formation of vortices.

The results obtained in the studies confirm why patients with larger bifurcation angle are more susceptible to the occurrence of plaques in the arteries. The investigations disregarded a number of variables, such as incorrect blood work, patient's lifestyle, thickness of the walls or the pulsating nature of the flow. These variables were disregarded because the authors focused on achieving an independent impact of bifurcation angle on the flow. Therefore other parameters of possible impact on the flow were omitted or simplified. The presented study results converge with the cases observed in practice – the largest group of patients with diagnosed deposits in the artery have the artery of the angle in excess of 50°. The points where deposits are formed very often occur near the bulb on the side of the internal artery, which is also confirmed by the performed studies. Based on the above prerequisites, a mechanically related confirmation was obtained as to why people of large carotid artery bifurcation angle



are more exposed to stenosis.

The performed studies are a starting point for the development of a carotid artery geometry database planned in the future. The database will include the geometry groups that increase the probability of deposits. A person exposed to stenosis will have an opportunity to take proactive measures. Thanks to the combination of engineering practice related to flow modeling and medical practice related to cardiovascular surgery, biochemistry and biomechanics, numerous issues, yet to be solved, can be explained. The results may significantly contribute to the development of prophylactics and improvement of the treatment of cardiovascular disease.

## REFERENCES

- [1] van Steenhoven, A.A.; van de Vosse, F.N. *Experimental and numerical analysis of carotid artery blood flow*, Blood Flow in Large Arteries: Applications to Atherogenesis and Clinical Medicine. Monogr Atheroscler. Basel, Karger, vol 15, pp 250-260, 1990.
- [2] Payam B. Bijari, Bruce A. Wasserman, David A. Steinman *Carotid Bifurcation Geometry Is an Independent Predictor of Early Wall Thickening at the Carotid Bulb*, Stroke, 2014.
- [3] C K Zarins, D P Giddens, B K Bharadvaj, V S Sotturrai, R F Mabon and S Glagov *Carotid bifurcation atherosclerosis. Quantitative correlation of plaque localization with flow velocity profiles and wall shear stress*, Journal of the American Heart Association, 1983.
- [4] Hong Yang Wang, Long Shan Liu<sup>1</sup>, Hai Ming Cao, Jun Li, Rong Hai Deng, Qian Fu<sup>1</sup>, Huan Xi Zhang, Ji Guang Fei<sup>1</sup>, Chang Xi Wang *Hemodynamics in Transplant Renal Artery Stenosis and its Alteration after Stent Implantation Based on a Patient specific Computational Fluid Dynamics Model*, Chinese Medical Journal, Volume 130 Issue 1 2017.
- [5] Gharahi H., Zambrano B., Zhu D. *Computational fluid dynamic simulation of human carotid artery bifurcation based on anatomy and volumetric blood flow rate measured with magnetic resonance imaging*, Int J Adv Eng Sci Appl Math, 2016.
- [6] João Pedro Carvalho Rêgo de Serra e Moura *Analysis and Simulation of Blood Flow in the Portal Vein with Uncertainty Quantification*, Master Thesis on Aerospace Engineering, 2011.
- [7] [https://www.sharcnet.ca/Software/Fluent6/html/ug/main\\_pre.htm](https://www.sharcnet.ca/Software/Fluent6/html/ug/main_pre.htm)
- [8] [https://www.cfd-online.com/Wiki/SST\\_k-omega\\_model#Specific\\_Dissipation\\_Rate](https://www.cfd-online.com/Wiki/SST_k-omega_model#Specific_Dissipation_Rate)
- [9] F.O. Ribeiro, M.J. Gómez-Benito, J. Folgado, P.R. Fernandes, J.M. García-Aznar. *Computational model of mesenchymal migration in 3D under chemotaxis*. Computer Methods in Biomechanics and Biomedical Engineering, **20**(1), 59-74, 2017.
- [10] Ji Young Moon, Dae Chul Suh, Yong Sang Lee, Young Woo Kim, Joon Sang Lee *Considerations of Blood Properties, Outlet Boundary Conditions and Energy Loss Approaches in Computational Fluid Dynamics Modeling*, Neurointervention Vol. 9, Issue 1, 2014.
- [11] Mark W. Siebert and Petru S. Fodor *Newtonian and Non-Newtonian Blood Flow over a Backward Facing Step – A Case Study*, excerpt from: Proceedings of the COMSOL Conference in Boston, 2009.
- [12] Wasilewski J., Kiljański T. *Biomechaniczna przyczyna miażdżycy*, Monografie Politechniki Łódzkiej, 2011.
- [13] Prosnak W. *Mechanika Płynów tom I*, Państwowe Wydawnictwo Naukowe, 1970.